General-relativistic approach to the nonlinear evolution of collisionless matter

Sabino Matarrese and Ornella Pantano
Dipartimento di Fisica "Galileo Galilei," Università di Padova, via Marzolo 8, I-35131 Padova, Italy

Diego Saez
Departamento de Fisica Teorica, Universidad de Valencia, Burjassot, Valencia, Spain
(Received 14 October 1992)

A new general-relativistic algorithm is developed to study the nonlinear evolution of scalar (density) perturbations of an irrotational collisionless fluid up to shell crossing, under the approximation of neglecting the interaction with tensor (gravitational-wave) perturbations. The dynamics of each fluid element is separately followed in its own inertial rest frame by a system of twelve coupled first-order ordinary differential equations, which can be further reduced to six under very general conditions. Initial conditions are obtained in a cosmological framework, from linear theory, in terms of a single gauge-invariant potential. Physical observables, which are expressed in the Lagrangian form at different times, can be traced back to the Eulerian picture by solving supplementary first-order differential equations for the relative position vectors of neighboring fluid elements. Similarly to the Zel'dovich approximation, in our approach the evolution of each fluid element is completely determined by the local initial conditions and can be independently followed up to the time when it enters a multistream region. Unlike the Zel'dovich approximation, however, our approach is correct also in three dimensions (except for the possible role of gravitational waves). The accuracy of our numerical procedure is tested by integrating the nonlinear evolution of a spherical perturbation in an otherwise spatially flat Friedmann-Robertson-Walker universe and comparing the results with the exact Tolman-Bondi solution for the same initial profile. An exact solution for the planar symmetric case is also given, which turns out to be locally identical to the Zel'dovich solution.

PACS number(s): 98.80.Bp, 04.20.Jb

I. INTRODUCTION

The dynamics of a system of particles having negligible nongravitational interactions, i.e., of a self-gravitating *collisionless* fluid, is of extreme importance in cosmology; this is in fact a well-motivated and widely applied approximation when dealing with the evolution of both cold and hot dark matter components. This problem is usually approached with different techniques, depending on the specific application. For instance, the evolution of small-amplitude disturbances of a Friedmann-Robertson-Walker (FRW) background is followed by analytical methods: Among these are the metric perturbation approach, originally due to Lifshitz [1], the fluid-flow approach initiated by Hawking [2], and the gauge-invariant method pioneered by Bardeen [3]. In the latter case, one relates physical observables to quantities which are invariant under changes of the map between the physical (perturbed) and the background (unperturbed) space-time. Specific perturbative treatments exist for the collisionless case or for the case of a mixture of a general perfect fluid with a collisionless gas (e.g., Ref. [4] and references therein). A post-Newtonian-type approximation has been followed by Futamase [5] to describe the dynamics of a clumpy universe. The nonlinear evolution in cases where some symmetries are present can sometimes be followed analytically: Typical examples are the spherical top-hat model for the Newtonian case (e.g., Ref. [6]) and the Tolman-Bondi (TB) solution [7] in general relativity (GR). A number of semianalytical treatments exist for the mildly nonlinear evolution of perturbations in Newtonian theory, such as the celebrated Zel'dovich approximation [8] and more recent refinements [9,10] or alternative approximations [11–13]. The most general problem of studying the fully nonlinear dynamics of a self-gravitating collisionless fluid can, however, only be followed by numerical techniques, such as N-body codes (e.g., Ref. [14]). A numerical fluid model for the nonlinear evolution of density fluctuations has been also proposed [15]. A large effort has been spent in the literature to analyze the spherical case in connection to the establishing of a self-similar regime both in the Newtonian [16] and GR cases [17]. The role of small deviations from spherical symmetry has also been investigated in this respect [18].

One can generally say that the following attitude has been followed so far in the literature on cosmological issues: A GR approach has been applied either in connection with the linear perturbation problem on large scales or when dealing with symmetric solutions of Einstein's equations; the most general nonlinear case, where no symmetries are present, is instead usually treated within Newtonian theory (in expanding coordinates). Newtonian mechanics is indeed expected to apply in regions small compared to the Hubble radius but large compared to the typical Schwarzschild radii of collapsing bodies; the universe outside these regions only affects the dynamics through tidal interactions (e.g., Ref. [6]). Relativistic

effects could then be relevant either in connection with structures extending over very large scales or with high bulk motions. Although, at present, the biggest coherent structures which have been observed have size of about one order of magnitude below the horizon scale and typical peculiar velocities are largely nonrelativistic, it can nevertheless be useful to have a general formalism able to describe correctly structures on even larger scales. Moreover, we believe that having a fully relativistic treatment of the evolution of structures in the Universe able to describe the nonlinear regime is itself an important theoretical issue.

We propose here a GR approach to the nonlinear evolution of scalar perturbations of a pressureless fluid. Our main assumptions are the absence of vortical motions and the disregarding of gravitational-wave interactions with the rest of the system. The kind of initial conditions we assume (only scalar modes present) is consistent with the predictions of inflation, an epoch of accelerated expansion in the early Universe when curvature fluctuations have been created in a causal way. Scalar perturbation modes arise from zero-point quantum fluctuations of the field driving inflation and are subsequently magnified by the accelerated Universe expansion to cosmologically relevant scales (e.g., Ref. [19] and references therein). Inflation also predicts that vortical perturbations either exactly vanish or have extremely small amplitude (e.g., Ref. [20] and references therein). As far as gravitational waves are concerned, the situation is as follows: A stochastic background of gravitons is created during inflation, whose rms amplitude at the Hubble-radius crossing can be comparable to that of density perturbations (e.g., Ref. [21] and references therein). Alternative mechanisms also exist for generating such a gravitational-wave background on large scales. Inside the Hubble radius, gravitational waves are redshifted and diluted by the universe expansion unless they are able to interact with the matter. If, as in our case, the matter content is described by a perfect fluid, no interactions occur at the linear level, so that these primordial gravitons freely propagate in the space-time generated by the surrounding matter. Moreover, no Jeans-like instability exists for tensor modes, and so, if these waves have small amplitude at early times, they will remain so at later times. The only possible interactions with matter may occur when density perturbations become large and nonlinear structures start to form. Because of these facts, we believe that disregarding the role of gravitational waves in large-scale structure evolution is a very good approximation.

Of course, one could exploit to a larger extent the irrotational character of our fluid motions: A single scalar potential would in fact allow a complete description of the fluid properties in a given metric (e.g., Ref. [22] and references therein), although some care is required when dealing with a fluid of dust. Newtonian calculations show that the overall dynamics of a self-gravitating pressureless fluid can indeed be described in terms of a single scalar variable (which could be identified either with the velocity potential or with the peculiar gravitational one) up to the time of the first shell crossing [23]. The GR problem is, however, complicated by the presence of the metric tensor: It is not at all obvious that a single potential can be used to describe the space-time geometry created by a fluid of dust deeply into the nonlinear regime. Also, because of this problem, we decided to avoid using scalar potentials and followed the fluid and space-time dynamics in terms of more direct quantities: the density, the expansion scalar, the shear tensor, and the tidal force one. In terms of these variables, the GR problem is reduced, for each fluid element, to first-order time-evolution equations. No spatial gradients appear in these equations provided one refers to the rest frame of observers comoving with the fluid; the absence of nongravitational interactions ("collisions") implies that these observers freely fall in the gravitational field created by the fluid, while the equivalence principle ensures that they do not feel gravity locally. General relativity therefore proves an economic way to account for the mutual gravitational interactions among different fluid elements without the need of simultaneously evolving all of them. However, as soon as the first caustics form, multistream regions appear and nonlocal effects start to play a relevant role in the subsequent evolution of these regions. It is worth noting the strong similarity between our method and the Zel'dovich approximation: In both cases the evolution of each fluid element is completely determined by the local initial conditions and can be independently followed up to the time when it enters a multistream region. Note, however, that our method is exact (except for having disregarded gravitational waves) in the most general three-dimensional case, while the Zel'dovich approximation is only exact for one-dimensional perturbations (where we shall in fact refer to it as Zel'dovich *solution*).

Because of our choice of fluid variables and reference frame, our method is a Lagrangian one: At the end of our calculations, physical observables are known in the rest frame of each fluid element. The next step is then to reconstruct the Eulerian density and peculiar velocity fields on suitable spacelike hypersurfaces. As we will show, this is indeed possible by integrating additional first-order equations to follow the relative displacement of neighboring elements. It would be interesting to compare our GR approach with the approximate solutions obtained by Buchert [24] by a Lagrangian approach within the Newtonian framework. A Lagrangian approach has also been recently used by Moutarde *et al.* [11] (see also Ref. [25]).

The plan of the paper is as follows. Section II introduces the equations which govern the relativistic dynamics of a self-gravitating collisionless fluid and defines our main approximations. Section III presents our algorithm for obtaining physical initial conditions, performing the integration of dynamical equations, and providing the final Eulerian representation of the results. Section IV deals with the evolution of a spherical perturbation: The results of numerical integrations are compared with exact Tolman-Bondi solutions in order to check the accuracy of our numerical method. Section V gives an exact solution of our set of equations for the particular case of planar symmetry. Section VI contains a general discussion of

the results.

We use the signature $(-,+,+,+)$; latin indices refer to space-time coordinates, (0,1,2,3), greek indices to spatial ones, (1,2,3). Units are such that the speed of light is 1.

II. RELATIVISTIC DYNAMICS OF SELF-GRAVITATING DUST

In this section we shall introduce the equations which govern the dynamics of a collisionless perfect fluid in GR. The dynamical equations are written in terms of observable fluid quantities (such as density, shear, etc.) and other tensor quantities which directly describe the space-time curvature (instead of the metric tensor). A complete treatment of the problem, as well as a full derivation of the equations presented here, can be found in the classical review by Ellis [26].

The relativistic dynamics of a collisionless (i.e., with vanishing pressure) self-gravitating perfect fluid is determined by Einstein's field equations and by the continuity equations for the matter stress-energy tensor $T_{ab}=\rho u_a u_b$, where ρ is the energy density and u^a the four-velocity of the fluid, such that $u^a u_a=-1$. It is also useful to define the spatial projection tensor $h^{ab}\equiv g^{ab}+u^a u^b$, for which $h_{ab}u^b=0$. By differentiating the velocity field, one obtains the tensor $v_{ab}\equiv h_a{}^c h_b{}^d u_{c;d}$, for which $v_{ab}u^b=0$, and the *acceleration* vector $\dot{u}^a\equiv u^a{}_{;b}u^b$, which is also spacelike, $\dot{u}^a u_a=0$, as it follows from the normalization condition. An overdot denotes convective differentiation with respect to the proper time t of fluid particles, namely, for a general n-index tensor, $\dot{A}_{a_1 a_2\cdots a_n}=A_{a_1 a_2\cdots a_n;b}u^b$.

Being flow orthogonal, the tensor v_{ab} has only nine independent components: Its antisymmetric part defines the *vorticity* tensor $\omega_{ab}\equiv v_{[ab]}$ (where the square brackets denote antisymmetrization, while parentheses denote symmetrization). Because of its antisymmetric character, the latter tensor has only three independent components which correspond to the vorticity vector $\omega^a=\frac{1}{2}\eta^{abcd}u_b\omega_{cd}$, where η_{abcd} is the completely antisymmetric four-index tensor. Equivalently, $\omega_{ab}=\eta_{abcd}\omega^c u^d$. The vorticity components describe rigid rotations of fluid elements with respect to a locally inertial rest frame. One has two more relevant quantities: the trace of the tensor v_{ab}, called the *volume-expansion* scalar $\Theta\equiv v^a{}_a$, and its symmetric and traceless part $\sigma_{ab}\equiv v_{(ab)}-\frac{1}{3}\Theta h_{ab}$, called the *shear* tensor. From the volume expansion scalar, giving the local rate of isotropic expansion (or contraction), one can also define a length scale l by the equation $\Theta=3\dot{l}/l$, which would just correspond to the scale factor $a(t)$ of homogeneous and isotropic FRW models; in that particular case, $\Theta=3H$, where $H(t)$ is Hubble's constant. The shear tensor, on the other hand, describes a pure straining in which a spherical fluid volume is distorted into an ellipsoid with axis lengths changing at rates determined by the three $\sigma^a{}_b$ eigenvalues σ_1, σ_2, and $\sigma_3=-(\sigma_1+\sigma_2)$. The vanishing trace condition implies that this deformation leaves the fluid volume invariant, while, in the absence of vorticity, the principal axes of the shear tensor keep their direction fixed during the evolution in a local inertial rest frame.

The fluid acceleration is only caused by pressure gradients, and so, in our case,

$$\dot{u}^a=0\ . \tag{2.1}$$

In the absence of pressure, *each fluid element moves along a geodesic.* In our pressureless case, the continuity equations for the *energy density* ρ and for the particle-number density take the same form, the two quantities being directly proportional. One has

$$\dot{\rho}=-\rho\Theta\ , \tag{2.2}$$

which, if integrated along a world line γ, gives the constancy of the product ρl^3 (conservation of rest mass). The expansion scalar satisfies the *Raychaudhuri equation*

$$\dot{\Theta}=\Lambda-\tfrac{1}{3}\Theta^2+2(\omega^2-\sigma^2)-4\pi G\rho\ , \tag{2.3}$$

where G is Newton's constant and we have introduced the *cosmological constant* Λ and the scalars $\omega^2\equiv\omega^a\omega_a=\frac{1}{2}\omega^{ab}\omega_{ab}$ and $\sigma^2\equiv\frac{1}{2}\sigma^{ab}\sigma_{ab}$. Note that in the homogeneous and isotropic case, $\omega_{ab}=\sigma_{ab}=0$ and the latter equation reduces to the familiar Friedmann one $3(\dot{H}+H^2)=-4\pi G\rho+\Lambda$. The vorticity vector evolves according to

$$\dot{\omega}^a=-\tfrac{2}{3}\Theta\omega^a+\sigma^a{}_b\omega^b\ . \tag{2.4}$$

The shear is determined by the equation

$$\dot{\sigma}_{ab}=-\sigma_{ac}\sigma^c{}_b-\omega_a\omega_b+\tfrac{1}{3}h_{ab}(2\sigma^2+\omega^2)-\tfrac{2}{3}\Theta\sigma_{ab}-E_{ab}\ , \tag{2.5}$$

where $E_{ac}\equiv C_{abcd}u^b u^d$ is the *electric* part of the Weyl or *conformal* tensor C_{abcd} (the latter being the part of the Riemann curvature not determined by local sources, which can be taken as representing the free gravitational field); $E^a{}_b$ is also called the *tidal force field,* since it contains that part of the gravitational field which describes tidal interactions; it is symmetric, traceless, and flow orthogonal, $E_{ab}u^b=0$. Tidal forces act on the fluid flow by inducing shear distortions. The tensor $E^a{}_b$ can be diagonalized by going to its principal axes (which do not generally coincide with those of the shear tensor), with eigenvalues E_1, E_2, and $E_3=-(E_1+E_2)$.

From the Weyl tensor, one defines another tensor, its *magnetic* part $H_{ac}=\frac{1}{2}\eta_{ab}{}^{gh}C_{ghcd}u^b u^d$. The tensor H_{ab} (which is also symmetric, traceless, and flow orthogonal) contains the part of the gravitational field which describes *gravitational waves.* Actually, gravitational waves are represented by the transverse traceless parts of E_{ab} and H_{ab}, satisfying $h^{bc}E_{ab;c}=0$ and $h^{bc}H_{ab;c}=0$ (e.g., Ref. [27]). While the tidal force field has a straightforward Newtonian analogue, which can be written in terms of derivatives of the gravitational potential, the magnetic part H_{ab} has no Newtonian counterpart. The important point is that, while in Newton's theory the gravitational potential is usually determined through a constraint equation, namely, Poisson's equation, in GR both E_{ab} and H_{ab} can be calculated by solving suitable evolution equations.

In what follows we shall make an important approximation, which will greatly simplify our system of equations, namely, *we shall neglect the influence of H_{ab} on the evolution of the tidal force field E_{ab}*. For initially scalar perturbations of an irrotational perfect fluid, this amounts to neglecting the interaction of gravitational waves (tensor modes) with the system. This approximation, together with the absence of pressure in the fluid, implies that no explicit spatial gradients (i.e., not included in total derivatives) are present in the evolution equations. We note that a similar approximation has been applied to follow the nonlinear evolution of long-wavelength metric fluctuations during inflation [28]. In such a simplified case, the tidal force field evolves according to

$$\dot{E}_{ab} = -h_{ab}\sigma^{cd}E_{cd} - \Theta E_{ab} + E_{c(a}\omega_{b)}{}^{c} + 3E_{c(a}\sigma_{b)}{}^{c} - 4\pi G\rho\sigma_{ab} \ . \tag{2.6}$$

Besides the evolution equations [Eqs. (2.1)–(2.6)], there are several *constraint equations* that our variables have to satisfy. These equations will be automatically satisfied at any time during the evolution provided we consistently set up our initial conditions: This will be easily done by building up the initial values of all our scalars, vectors, and tensors within linear theory.

The great advantage of having assumed zero pressure and neglected the interaction with gravitational waves is that *no spatial derivatives appear explicitly in the equations.* There are in the general case, however, spatial derivatives hidden in the *convective* time differentiation of tensors (the overdot), because of the presence of the affine connection Γ^{a}_{bc} in covariant derivatives. In fact, while for a scalar quantity convective differentiation and simple differentiation can be made to coincide, provided one uses a reference frame comoving with the fluid, this no longer holds for a vector such as u^{a} or for two-index tensors such as σ_{ab} and E_{ab}. In all our previous equations, another tensor variable is always present, together with its partial derivatives, the metric tensor, which satisfies the evolution equation

$$\dot{g}_{ab} = 0 \ . \tag{2.7}$$

In our case of zero acceleration, this also implies $\dot{h}_{ab} = 0$.

Before concluding this section, let us briefly discuss the main limitations of our approach.

First, the assumption of vanishing pressure: This is a key one, since it allows to follow different fluid trajectories independently. However, as we have already mentioned in the Introduction, this is a good description in most cosmological applications.

Second, the assumption of neglecting H_{ab}: Although this is the only actual approximation we have made, we consider it as a very minor limitation in most cosmological applications of the method. Its validity can be, however, verified by calculating this tensor through the constraint equation

$$H_{ab} = -h_{a}{}^{t}h_{b}{}^{s}(\omega_{(t}{}^{d;c} + \sigma_{(t}{}^{d;c})\eta_{s)fdc}u^{f} \tag{2.8}$$

and evaluating how much this would affect the evolution of E_{ab} [this would, for course, require the complete form of the equations, including terms containing H_{ab} which are not reported here (e.g., Ref. [26])]. The general case of exact solutions of Einstein's equation with $H_{ab} = \omega_{ab} = 0$ is considered by Barnes and Rowlingson [29].

We also assume zero vorticity for the fluid, $\omega_{ab} = 0$. According to Kelvin's circulation theorem, in the absence of dissipation, vorticity is conserved along each fluid trajectory; in particular, a fluid with vanishing initial vorticity will forever remain irrotational. However, for a collisionless fluid, such a property breaks down after caustic formation: A vorticity component is created in multistream regions, simply because the local Eulerian velocity field takes contributions from different Lagrangian fluid elements at the same position. On the other hand, this problem can be avoided if one restricts the analysis to suitably large scales, where stream lines evolve without crossing each other. These points are discussed in detail by Dekel, Bertschinger, and Faber [30] for the Newtonian case. It is nevertheless important to stress that our method does not in principle require irrotational motion. This assumption is, however, useful in order to reduce the number of equations and dynamical variables. It also eases the construction of spatial hypersurfaces and simplifies the final interpretation of the results.

III. GENERAL-RELATIVISTIC APPROACH

In this section we develop a general method to study the evolution of a self-gravitating collisionless perfect fluid, which is based on the GR formalism described in Sec. II. Linear approaches based on the same formalism have been given by Hawking [2] and Olson [31] and more recently by Lyth and co-workers [32], while a gauge-invariant formulation has also been considered [33,34]. Our method can be divided into four main steps: (i) An initial grid is defined and only the world lines of fluid elements corresponding to the nodes are considered; (ii) for each world line γ, the most suitable coordinate system is chosen; (iii) initial conditions for the integration of dynamical equations are assumed and the integration is performed along each world line; (iv) finally, the results of the integration along all world lines of the nodes are interpreted. Points (i)–(iv) are analyzed in detail in Secs. III A–III D below.

A. Initial grid and its evolution

In the space-time created by an irrotational pressureless perfect fluid, the time coordinate t can be defined in such a way that any hypersurface $t = \text{const}$ is orthogonal to the world lines of the fluid elements at any point and the variation of t along each world line coincides with the proper time variation along it. The time coordinate of the *comoving time-orthogonal gauge* (e.g., Ref. [3]), which will be introduced in Sec. III C, has precisely these properties: This is because comoving hypersurfaces (orthogonal to the energy flow) and synchronous ones (orthogonal to geodesics) coincide in the absence of pressure gradients. Thus, in such a gauge, if the initial grid is located

on the hypersurface $t=t_{\rm in}$, orthogonal to the flow lines, and the integration of the equations is carried out over the same proper time interval Δt for every node, the end points of the integrations will lie on the final hypersurface $t=t_{\rm in}+\Delta t$, also orthogonal to the flow lines.

A measure of the curvature of any hypersurface $t=$const is provided by the three-dimensional Ricci scalar (e.g., Ref. [26])

$$\mathcal{R}^{(3)}=-\tfrac{2}{3}\Theta^2+2\sigma^2+16\pi G\rho+2\Lambda\ . \tag{3.1}$$

The spatial distance between two arbitrary neighboring nodes P and Q of the initial grid will be assumed to be much smaller than $1/[|\mathcal{R}^{(3)}(t_{\rm in})|]^{1/2}$, so that the quantities 0, $x^1_Q-x^1_P$, $x^2_Q-x^2_P$, and $x^3_Q-x^3_P$ can be considered as the components of the (infinitesimal) *relative position vector* ξ^a, tangent to the hypersurface $t=t_{\rm in}$ at P. More in general $\xi_a u^a=0$. These neighboring points are finally mapped into the points $P(t)$ and $Q(t)$ on the final hypersurface $t=t_{\rm in}+\Delta t$, whose curvature is $\mathcal{R}^{(3)}(t)$. When, for a given Δt, the distance $\delta l\equiv(h_{ab}\xi^a\xi^b)^{1/2}$ between two neighboring points becomes larger than $1/[|\mathcal{R}^{(3)}(t)|]^{1/2}$ in some region, one can increase the initial grid resolution and perform the integration only for the fluid elements corresponding to the new grid points. The vector ξ^a evolves according to the well-known equation (e.g., Ref. [26])

$$\dot{\xi}^a=\tfrac{1}{3}\Theta\xi^a+(\omega^a{}_b+\sigma^a{}_b)\xi^b\ , \tag{3.2}$$

which will be only considered here in the irrotational case $\omega_{ab}=0$.

The values of the ξ^a components depend on the coordinate system. In spherically symmetric cases, such as the TB one of Sec. IV, each Cartesian axis passing through the center of symmetry, say, x^3, is just one possible radial direction, and so a one-dimensional grid along that axis is enough. Thus ξ^1 and ξ^2 can be taken to vanish identically and δl becomes the radial distance between neighboring nodes. A number of simplifications will generally occur in symmetric cases. Even in applications of the method to symmetric cases, it is important that, at the initial time, each quantity be calculated in the comoving time-orthogonal gauge: The grid can be then built on a hypersurface $t=t_{\rm in}$ orthogonal to the flow lines and the integrations carried out over the same Δt for each node.

The system formed by Eqs. (2.2)–(2.6) with $\omega_{ab}=0$ (hereafter system A) is a set of 12 coupled partial differential equations involving 12 independent variables: σ_{ab} (five independent variables), E_{ab} (five independent variables), plus ρ and Θ. As we shall see in Sec. III C, this system can be reduced to a set of six equations for the same number of unknowns by going to the simultaneous local principal axes of the shear and tidal force fields. The three supplementary differential equations (3.2) have to be solved next to compute the components of each vector ξ^a needed to reconstruct the final grid. For a cubic grid with N_g^3 nodes, one would then need to solve $6N_g^3$ first-order equations to obtain the dynamical variables plus $3(N_g-1)(N_g^2+N_g+1)$ extra ones (still of first order) for the relative-position-vector components, this being the minimum number required to fix rigidly the evolved grid.

B. Coordinate system

In the absence of pressure, any world line of the fluid corresponds to a freely falling "observer" evolving in a purely gravitational field. Thanks to the weak equivalence principle, such an observer does not feel gravity locally. This means that there are comoving coordinate systems where the affine connection vanishes all along γ. In these locally *inertial rest frames* (IRF's), one has

$$\dot{A}_{a_1a_2\cdots a_n}=\frac{d}{dt}A_{a_1a_2\cdots a_n}=\frac{\partial}{\partial t}A_{a_1a_2\cdots a_n} \tag{3.3}$$

and the overdot stands for a derivative with respect to the proper time t of the observer γ. Thus, in the IRF of γ, the system formed by A plus Eq. (3.2) becomes a set of ordinary first-order differential equations with t as the independent variable. From Eqs. (2.1) and (2.7), we then conclude that the four-velocity and the metric do not change in the IRF of γ. In some IRF's this constant metric takes a Minkowskian form. These *local Minkowskian frames* (LMF's) are therefore the best coordinates to integrate our system, which is therefore reduced to a system of ordinary first-order differential equations without spatial derivatives and can be integrated by standard numerical methods.

C. Initial conditions and time evolution

System A is integrated along each world line of the fluid, indeed, along the world lines passing through the nodes of the initial grid. For each line γ, the integration is carried out in a different coordinate system, namely, in one LMF of γ, but the initial conditions at different points are not independent because quantities such as the tidal force field have a nonlocal dependence on the mass distribution. Note, in fact, that E_{ab}, in the Newtonian limit, reduces to $E_{\alpha\beta}=\phi_{,\alpha\beta}-\frac{1}{3}\delta_{\alpha\beta}\nabla^2\phi$ (commas denote partial spatial derivatives, while $\delta_{\alpha\beta}$ stands for the Kronecker symbol), where the gravitational potential ϕ is determined by the total mass distribution via Poisson's equation $\nabla^2\phi=4\pi G\rho-\Lambda$ and suitable boundary conditions. The initial conditions at different grid points must be solutions of Einstein and fluid-conservation equations, in order to ensure the compatibility between the initial conditions at each grid point and the global structure of the system. Two types of solutions can be used to fix the initial conditions: solutions of the linearized cosmological equations and exact symmetric solutions. Any cosmologically relevant energy perturbation was indeed linear at sufficiently early times; thus, linearized solutions allow one to study completely general perturbations. On the other hand, exact symmetric solutions, such as the TB one, can be useful in order to test the accuracy of our numerical algorithm. This will be done in Sec. IV. In addition, in Sec. V we will show how our system reproduces the well-known Zel'dovich solution [8] for a planar symmetric perturbation.

Linear perturbations on a FRW background are constructed by using the gauge-invariant Bardeen formalism [3]. Scalar modes defined in this formalism imply vanishing initial values for the tensor ω_{ab} and H_{ab}. Furthermore, the inclusion of small-amplitude tensor modes (gravitational waves) is still compatible with our general assumptions. A matter-dominated and spatially flat (i.e., Einstein–de Sitter) FRW background with vanishing cosmological constant is introduced. The line element is $ds^2=-dt^2+a^2\delta_{\alpha\beta}dx^\alpha dx^\beta$, whose scale factor grows with the cosmic time as $a(t)=a_{\rm in}(t/t_{\rm in})^{2/3}$. The background density is $\rho_B=1/6\pi Gt^2$, while $\Theta_B=2/t$. A generalization to the open and closed matter-dominated FRW cases, as well as the inclusion of a nonzero cosmological constant, is straightforward.

Since only scalar perturbations are actually relevant, perturbations of physical variables, scalars, and tensor components can be expressed as linear superpositions of scalar harmonics $Q_{\mathbf{k}}(\mathbf{x})$ with gauge-invariant, generally time-dependent, amplitudes labeled by the eigenvalues $\mathbf{k}$, these harmonics being defined as solutions of the scalar Helmholtz equation $\nabla^2 Q_{\mathbf{k}}=-k^2 Q_{\mathbf{k}}$ (e.g., plane waves).

1. Initial conditions in the comoving gauge

We can now define a linearly perturbed FRW line element in the comoving time-orthogonal gauge. It reads

$$ds^2=-dt^2+a^2(t)[\delta_{\alpha\beta}-2a(t)\varphi_{,\alpha\beta}(\mathbf{x})]dx^\alpha dx^\beta . \tag{3.4}$$

The scalar perturbations of the metric-tensor components have been written in terms of the single gauge-invariant variable φ, which is related to Bardeen's Φ_H by $\varphi\equiv-(3t_{\rm in}^2/2a_{\rm in}^3)\Phi_H$; the smallness of the perturbations is here monitored by the smallness of the initial scale factor $a_{\rm in}$. Although our general algorithm can work with arbitrary initial conditions, we restrict ourselves here only to the case of vanishing nongrowing modes. Instead of the curvature perturbation, or peculiar gravitational potential φ, which has the advantage of remaining constant in the linear regime, one could have referred to other variables such as the gauge-invariant density perturbation $\varepsilon_m=a\nabla^2\varphi$, corresponding to the true density fluctuation $\delta\equiv\delta\rho/\rho$ in our comoving, time-orthogonal gauge.

The variables involved in system A can be written in terms of φ as

$$\rho(\mathbf{x},t)=\frac{1}{6\pi Gt^2}[1+a(t)\nabla^2\varphi(\mathbf{x})] , \tag{3.5}$$

$$\Theta(\mathbf{x},t)=\frac{2}{t}\left[1-\frac{a(t)}{3}\nabla^2\varphi(\mathbf{x})\right] , \tag{3.6}$$

$$\sigma_\alpha{}^\beta(\mathbf{x},t)=-\frac{2a(t)}{3t}[\delta^{\beta\gamma}\partial_\alpha\partial_\gamma-\tfrac{1}{3}\delta_\alpha{}^\beta\nabla^2]\varphi(\mathbf{x}) , \tag{3.7}$$

$$E_\alpha{}^\beta(\mathbf{x},t)=\frac{2a(t)}{3t^2}[\delta^{\beta\gamma}\partial_\alpha\partial_\gamma-\tfrac{1}{3}\delta_\alpha{}^\beta\nabla^2]\varphi(\mathbf{x}) , \tag{3.8}$$

and $\sigma^0{}_0=\sigma^0{}_\alpha=E^0{}_0=E^0{}_\alpha=0$. The shear and tidal-force-field tensors, which identically vanish in the background, are already gauge invariant (e.g., Ref. [33]).

Owing to our choice of FRW model, the spatial curvature is zero in the background; then, at the linear level, Eq. (3.1) implies $\mathcal{R}^{(3)}_{\rm in}=(40a_{\rm in}/9t_{\rm in}^2)\nabla^2\varphi$.

General initial conditions are therefore completely defined by the choice of the potential $\varphi(\mathbf{x})$. These could be obtained, for instance, by a realization of a homogeneous and isotropic random (e.g., Gaussian) field in the region covered by the grid.

2. Initial conditions in locally Minkowskian coordinates

At a given node P of the initial grid, defining the world line γ, the initial conditions must be given in a LMF. These can be easily obtained from those in the comoving gauge. At this node the coordinate change (e.g., Ref. [35])

$$\bar{x}^a=B^a{}_b(x_P)(x^b-x_P^b)+\tfrac{1}{2}B^a{}_d(x_P)\Gamma^d_{bc}(x_P)(x^b-x_P^b)(x^c-x_P^c) , \tag{3.9}$$

with

$$\eta_{ab}B^a{}_c(x_P)B^b{}_d(x_P)=g_{cd}(x_P)$$

and η_{ab}, the Minkowski tensor, locally relates comoving coordinates to a LMF, where the metric becomes Minkowskian and the affine connection locally vanishes, $\bar{\Gamma}^a_{bc}(\bar{x}_P)=0$. Here the affine connection components are calculated from the metric (3.4). For each node P, one has a different change of the form of Eq. (3.9). It is well known that the quantities $B^a{}_b$ are defined up to a local Lorentz transformation. In particular, we can choose our new basis so that $B^0{}_0=1$ and $B^0{}_\alpha=B^\alpha{}_0=0$: In such a case, $\bar{u}_P^\alpha=0$ and the LMF coordinates $\bar{x}^a$ are comoving for the observer defined by P.

The spatial components $B^\alpha{}_\beta$ are specified up to a local spatial rotation. We shall fix them by requiring that the bases defined at different nodes be parallel among themselves. A set of parallel spatial axes can be obtained as follows. Starting from comoving coordinates, we can choose an arbitrary orthonormal basis $B^\alpha{}_\beta(x_O)$ in a given point O chosen as the origin. Given any other point P of the initial grid, we can choose an arbitrary path on the grid joining O to P. Then the basis $B^\alpha{}_\beta(x_O)$ can be parallel transported out to P along this path. This procedure is performed in the original comoving coordinates where the affine connection coefficients have been calculated from the metric (3.4) and the components of these parallel transported bases in each point P, $C^\alpha{}_\beta(x_P)$, are then given in comoving coordinates. By requiring that $B^\alpha{}_\beta(x_P)=C^\alpha{}_\beta(x_P)$, we have that the new basis, representing the LMF in P, is also parallel to that in the origin O.

3. Reduction to principal axes of the shear and tidal force tensors

An analysis of the initial conditions for system A shows that there is another preferred choice of spatial axes for the LMF in which the total number of equations and unknowns can be largely reduced. These correspond to the simultaneous principal axes of the shear and tidal

force fields at the initial time. These LMF's are related to the ones defined above by a simple local spatial rotation.

Since at the initial time $\sigma^{\alpha}{}_{\beta}$ and $E^{\alpha}{}_{\beta}$, computed in the comoving gauge, are both proportional to the symmetric tensor $\varphi_{,\alpha\beta}$, which is also responsible for the nondiagonal character of the perturbed metric, a local rotation from the comoving coordinates to the principal axes makes the perturbed line element locally diagonal too. Then a local transformation of the form (3.9) with diagonal $B^{\alpha}{}_{\beta}$ leads to LMF's with coordinate axes parallel to the principal ones. The latter transformation does not affect the components of the diagonalized mixed tensors $\alpha^{\alpha}{}_{\beta}$ and $E^{\alpha}{}_{\beta}$. The total transformation is described by the matrices $\Lambda^{\alpha}{}_{\beta}(\mathbf{x}, t_{\rm in})$, whose explicit form can be easily evaluated at each grid point.

At the initial time, one has the following independent eigenvalues for the shear,

$$\sigma_1(t_{\rm in}) = -\frac{2a_{\rm in}}{9t_{\rm in}}(2\lambda_1-\lambda_2-\lambda_3) ,$$
$$\sigma_2(t_{\rm in}) = -\frac{2a_{\rm in}}{9t_{\rm in}}(2\lambda_2-\lambda_1-\lambda_3) , \tag{3.10}$$

while for the tidal force field one has

$$E_1(t_{\rm in}) = \frac{2a_{\rm in}}{9t_{\rm in}^2}(2\lambda_1-\lambda^2-\lambda_3) ,$$
$$E_2(t_{\rm in}) = \frac{2a_{\rm in}}{9t_{\rm in}^2}(2\lambda_2-\lambda_1-\lambda_3) , \tag{3.11}$$

where $\lambda_{\alpha}(\mathbf{x}, t_{\rm in})$ are the eigenvalues of $\varphi_{,\alpha\beta}$, which should be evaluated at each grid pint.

Because of the absence of vorticity, these principal axes do not rotate in a LMF of γ, and so the shear and tidal force fields will both remain diagonal there at any successive time. In fact, from Eqs. (2.5) and (2.6), one can easily verify that the off-diagonal components remain zero if they were zero initially (see also Ref. [29]). The system of equations A is therefore reduced to the six first-order equations

$$\begin{aligned}
&\dot{\rho} = -\rho\Theta ,\\
&\dot{\Theta} = -\tfrac{1}{3}\Theta^2 - 2(\sigma_1^2+\sigma_2^2+\sigma_1\sigma_2) - 4\pi G\rho ,\\
&\dot{\sigma}_1 = -\tfrac{1}{3}\sigma_1^2 + \tfrac{2}{3}\sigma_2(\sigma_1+\sigma_2) - \tfrac{2}{3}\Theta\sigma_1 - E_1 ,\\
&\dot{\sigma}_2 = -\tfrac{1}{3}\sigma_2^2 + \tfrac{2}{3}\sigma_1(\sigma_2+\sigma_1) - \tfrac{2}{3}\Theta\sigma_2 - E_2 ,\\
&\dot{E}_1 = E_1(\sigma_1-\sigma_2) - E_2(\sigma_1+2\sigma_2) - \Theta E_1 - 4\pi G\rho\sigma_1 ,\\
&\dot{E}_2 = E_2(\sigma_2-\sigma_1) - E_1(\sigma_2+2\sigma_1) - \Theta E_1 - 4\pi G\rho\sigma_2 ,
\end{aligned} \tag{3.12}$$

with initial conditions given by Eqs. (3.5), (3.6) (note that $\nabla^2\varphi = \lambda_1+\lambda_2+\lambda_3$), (3.10) and (3.11).

The relative position vectors, written in the transformed coordinates $\zeta^{\alpha} = \Lambda^{\alpha}{}_{\beta}\xi^{\beta}$ evolve according to the equations

$$\dot{\zeta}^{\alpha} = (\sigma_{\alpha} + \tfrac{1}{3}\Theta)\zeta^{\alpha} , \tag{3.13}$$

where $\sigma_{\alpha} \equiv (\sigma_1, \sigma_2, -\sigma_1-\sigma_2)$ and no summation over the index α is understood.

To summarize, the main steps of this method are the following. Given the second derivatives of the initial peculiar gravitational potential $\varphi_{,\alpha\beta}$ at every grid point, one calculates its eigenvalues and eigenvectors. The local rotation to principal axes provides a simultaneous diagonalization of the metric, shear, and tidal force tensors. The reduced system (3.12) is then integrated along the world line of the fluid element defined at each grid point up to the final time. Also, the relative position vectors of different grid points are evolved in the rotated bases according to Eq. (3.13).

As we have already stressed above, the simultaneous diagonalization of the shear and tidal force fields is ensured by our choice of linear initial conditions and it is also fully consistent with nonlinear dynamics: no off-diagonal terms can develop in $\sigma^{\alpha}{}_{\beta}$ or $E^{\alpha}{}_{\beta}$ if they were not present in the initial conditions. On the other hand, if we had evolved the system in a general frame, where these two tensors are not initially diagonal, small numerical instabilities might develop, which would forbid simultaneous diagonalization at a later stage. One could argue that these instabilities mimic physical phenomena such as viscous forces, collisions, etc., which would be present in a less idealized situation. On the other hand, we do not expect these effects to become relevant before caustic formation, and so we believe that our diagonalized system allows a good description up to that epoch.

D. Interpretation of results: Eulerian picture

Since a different coordinate system has been used for each node of the grid, the results require interpretation. The value of a scalar does not depend on the coordinates; thus, for any node, the energy density $\rho = T_{ab}u^a u^b$ and the expansion $\Theta = u^a{}_{;a}$, obtained by numerical integration, represent the true physical quantities measured by freely falling observers with four-velocity u^a. The emerging description of the fluid flow represents a Lagrangian picture.

After numerical integration we are interested in the spatial distance among the final nodes and their peculiar velocities in order to reconstruct the Eulerian density and peculiar velocity field on the final hypersurface. Unfortunately, most of this information is stored in the tensor components of the shear and metric, i.e., not in scalar quantities. These components are not computed in a well-defined coordinate system independent of the assumed node. Thus a suitable method leading to the required information about positions and velocities is needed.

In the LMF attached to the nodes of the grid, the initial spatial bases have been chosen to be orthonormal. Moreover they are either parallel among themselves (our first choice) or easily related to parallel bases by local spatial rotations (our choice of axes parallel to the principal ones). These bases are parallel transported along the geodesics of the fluid particles; thanks to the absence of vorticity, no rotation, no gyroscopic precession is implied (e.g., Ref. [35]). As a consequence, the transported coordinate bases are also orthonormal at $t = t_{\rm in} + \Delta t$, for any Δt. Owing to the presence of curvature, however, these

bases are no longer parallel among themselves. Our final spatial bases can be, however, considered as quasiparallel, since the curvature induced by any cosmologically relevant perturbation remains small even in the strongly nonlinear regime. A relevant exception comes from caustics, where a shell-crossing singularity arises (e.g., Ref. [36]). This is, however, an artifact of having extrapolated our approximation down to zero distance, and it is reasonable to expect that, with a more realistic treatment of the fluid, this singular behavior might disappear. No simplification on the curvature has been assumed, neither in the initial conditions nor in the integrations; only in the three-dimensional representation of the final positions and velocities will the curvature on the $t=t_{\rm in}+\Delta t$ hypersurface be neglected. The deformation induced by this approximation is not expected to hide the main features of the matter distribution.

The relative position vectors and relative velocities among the nodes are generally obtained by integrating Eq. (3.2). If, in particular, the evolution has been followed in a frame with axes coinciding with the principal ones of the shear and tidal force fields, the relative position vectors are easily obtained in the initial locally comoving frame by inverting the matrix $\Lambda^{\alpha}{}_{\beta}$, namely, $\xi^{\alpha}(t)=(\Lambda^{-1})^{\alpha}{}_{\beta}\xi^{\beta}(t)$. One then obtains

$$\xi^{\alpha}=(\Lambda^{-1})^{\alpha}{}_{\beta}\Lambda^{\beta}{}_{\gamma}\xi^{\gamma}_{\rm in}\exp(f_{\beta}) , \tag{3.14}$$

where

$$f_{\beta}(t)=\int_{t_{\rm in}}^{t} dt'[\sigma_{\beta}(t')+\tfrac{1}{3}\Theta(t')] . \tag{3.15}$$

Similarly, the relative velocity between neighboring elements reads

$$V^{\alpha}\equiv\dot{\xi}^{\alpha}+(\Lambda^{-1})^{\alpha}{}_{\beta}\Lambda^{\beta}{}_{\gamma}\xi^{\gamma}_{\rm in}(\sigma_{\beta}+\tfrac{1}{3}\Theta)\exp(f_{\beta}) . \tag{3.16}$$

A Eulerian picture of the results can now be obtained as follows. A suitable node O is chosen as the origin of coordinates in the three-dimensional Euclidean space. In order to find Cartesian coordinates x^{α} of any other node S, a path connecting O to S is chosen on the grid and the quantities ξ^{α} corresponding to each pair of neighboring nodes of this path are added. If the approximation of neglecting the curvature was correct, the coordinates of any node S should be almost independent of the chosen path (one could also define the S coordinates as the mean of those obtained by several paths). The velocity of a given node S with respect to the origin O can be obtained by adding relative velocities V^{α} of neighboring nodes belonging to an arbitrary path OS; this sum can be performed according to the standard Euclidean rules; no relativistic corrections become necessary, since, in the cosmologically interesting cases, the typical velocities are expected to be much smaller than the speed of light, provided we deal with distances much smaller than the horizon size. To compute the velocities with respect to the background (i.e., the space-time obtained by spatially averaging over a comoving hypersurface at each time), two methods can be followed. The simplest method is to choose an origin at rest with the background and compute relative velocities with respect to it. The origin can be chosen to lie in a region far from an asymptotically vanishing inhomogeneity. In the spherically symmetric TB case discussed in the next section, the origin is the center of symmetry. The second method is general: It applies when the peculiar velocity of any node is unknown. In such a case, the origin can be located in a random set of nodes, the velocity of each node with respect to each origin is calculated, and, finally, the velocity of each node is defined as the average of its relative velocities with respect to all of the origins.

IV. TESTING THE METHOD WITH A SPHERICAL PERTURBATION

In this section we shall test the accuracy of our algorithm by numerically integrating the nonlinear evolution of a spherically symmetric perturbation in an otherwise spatially flat matter-dominated FRW space-time. The advantages of this example are that there is a known GR exact solution for this case, namely, the Tolman-Bondi metric [7], and that no gravitational waves arise during the evolution, and so our set of equations contains no approximations in such a special case. The TB solution has been recently applied by a number of authors to model large-scale structures such as large voids in the galaxy distribution or the great attractor region (e.g., Refs. [37,38]).

A. Tolman-Bondi space-time

Before describing our approach, let us review the TB solution. The TB line element can be written in comoving coordinates t, M, θ, ϕ as

$$ds^2=-dt^2+\frac{1}{\Gamma^2}\left[\frac{\partial R}{\partial M}\right]^2 dM^2+R^2(d\theta^2+\sin^2\theta\, d\phi^2) , \tag{4.1}$$

where $R=R(M,t)$ is a radial "Eulerian" coordinate,

$$\Gamma^2=1+f(M)=1+\left[\frac{\partial R}{\partial t}\right]^2-\frac{2GM}{R} , \tag{4.2}$$

and f represents the conserved specific energy of a shell of radius R.

The explicit form of the function $R(M,t)$ depends on the sign of f. Three cases can be distinguished.

(i) $f>0$:

$$\begin{aligned} &R=(GM/f)(\cosh\chi-\chi) , \\ &t-t_{*}(M)=(GM/f^{3/2})(\sinh\chi-\chi) . \end{aligned} \tag{4.3}$$

(ii) $f<0$:

$$\begin{aligned} &R=-(GM/f)(1-\cos\chi) , \\ &t-t_{*}(M)=(GM/|f|^{3/2})(\chi-\sin\chi) . \end{aligned} \tag{4.4}$$

(iii) $f=0$:

$$R=(9GM/2)^{1/3}[t-t_{*}(M)]^{2/3} . \tag{4.5}$$

The source of TB space-time is given by a spherically symmetric distribution of dust with mass density $\rho=1/4\pi R^2(\partial R/\partial M)$. According to Eq. (4.1), the radial

distance from the center to M, on the hypersurface $t=$const, is $D(M)=\int_0^M dM(1/\Gamma)(\partial R/\partial M)$, while the radial velocity of a fluid particle in M is

$$V_R=\frac{dD}{dt}=\int_0^M dM\frac{1}{\Gamma}\frac{\partial^2 R}{\partial M\,\partial t}\ .$$

Identifying the two quantities R and D (or $\partial R/\partial t$ and V_R) is meaningful only for small enough distances from the center. By assuming $\Gamma^2=1-\kappa r^2$, with $\kappa=1,0,-1$, $R=a(t)r$, and $M=4\pi\rho_B R^3/3$, with uniform ρ_B, the line element of Eq. (4.1) reduces to that for the closed, flat, and open FRW models, with scale factor $a(t)$. A FRW universe can then be considered as a special case of the TB one, and any cosmologically admissible TB solution must tend to a FRW universe as the spatial distance from the center of symmetry increases. Such a FRW space-time will be therefore referred to as the "background space-time." In this work the FRW background is taken to be a flat one.

The TB solution involves two arbitrary functions $t_*(M)$ and $f(M)$ to be determined from the initial profiles of two independent quantities. The remainder of this section is devoted to the description of the procedure used to obtain the final profiles of physical quantities from two initial profiles defining a particular realization of the TB solution.

A map Ξ from the TB space-time to the FRW one will be defined as follows: If a point P belongs to the background FRW space-time and a point Q belongs to the physical TB one, $P=\Xi(Q)$ if and only if P and Q have the same coordinates t,M,θ,ϕ. Since these coordinates are comoving in both space-times, Ξ actually defines a comoving gauge. The perturbation of any quantity A at a point Q in the physical space-time with respect to the same quantity in the background is defined as $\Delta A=A(Q)-A(\Xi(Q))$.

At the time $t_{\rm in}$, the density contrast is taken to be much smaller than unity, so that the TB solution describes a spherically symmetric perturbation superposed on FRW space-time. According to our previous discussion, the initial conditions can be fixed by assuming the initial profile $\Delta A(M,t_{\rm in})$ for two quantities. We consider the set formed by the density ρ and by $t_*(M)$ [$t_*(M)=0$ in FRW space-time]. The initial density profile is

$$\rho(M,t_{\rm in})=\rho_B(t_{\rm in})+\Delta\rho(M,t_{\rm in})\ ,$$

where $\rho_B(t_{\rm in})$ is the initial background density and the perturbation is assumed to be of the form

$$\Delta\rho(M,t_{\rm in})=\epsilon\rho_B(t_{\rm in})\{1+[R(M,t_{\rm in})/R_V]^2\}^{-1}\ , \qquad (4.6)$$

where the parameter ϵ determines the amplitude of the density contrast and R_V fixes the size of the inhomogeneity. The equation $t_*(M)=0$ defines the second independent profile.

The function $R(M,t_{\rm in})$ becomes implicitly defined by the equation

$$M=\frac{4\pi\rho_B(t_{\rm in})}{3}\{R^3+3\epsilon R_V^2[R-R_V\arctan(R/R_V)]\}\ . \qquad (4.7)$$

Given M, this equation can be numerically solved to obtain $R(M,t_{\rm in})$ and then Eq. (4.6) can be used to get $\Delta\rho(M,t_{\rm in})$. The function $f(M)$ can be found from the initial profiles of ρ and t_* as follows. Replacing $t_*(M)=0$ in Eq. (4.3), one obtains, for $f>0$,

$$t_{\rm in}=(GM/f^{3/2})\{[(Rf/GM)^2+2(Rf/GM)]^{1/2}-\operatorname{arccosh}[1+(Rf/GM)]\}\ . \qquad (4.8)$$

In a similar way, we obtain two more equations for $t_{\rm in}$ from Eq. (4.4), for $f<0$, and from Eq. (4.5), for $f=0$, whose explicit form will not be reported here. The function $f(M)$ can be obtained from one of these three equations: For a given M, only one of them has a solution, which can be numerically calculated. The profile $R(M,t_{\rm in})$, defined by Eq. (4.7), can then be replaced into that equation to obtain $f(M)$, which finally determines our TB solution. One can then compute R, $\partial R/\partial t$, $\partial R/\partial M$, $\partial^2 R/\partial M\,\partial t$, and other functions of M and t. The TB metric, the density, the radial distance from the center, the radial velocity of each shell of fluid, the expansion, and all the physically relevant quantities can be calculated at any time.

According to Ref. [39], the necessary and sufficient conditions which ensure the absence of shell crossing in the $t_*(M)=0$ case are $df/dR>0$, for $f\geq 0$, and $df/dR\geq 2f/3M$, for $f<0$. These conditions have been numerically verified in our case.

B. Initial conditions from the TB solution

The application of the general method described in Sec. III to the present case of spherical symmetry requires initial conditions in a comoving gauge and a one-dimension radial grid on the hypersurface $t=t_{\rm in}$. Cartesian coordinates x^α must be used both in the physical TB space-time and in the FRW background. The TB solution has been completely determined and its initial conditions have been fixed by using the comoving gauge Ξ and the coordinates t,M,θ,ϕ both in TB and FRW space-times. A change of coordinates in both space-times does not change the gauge Ξ, and so the required comoving gauge with Cartesian coordinates on the background hypersurfaces $t=$const is obtained.

The grid is taken along the x^3 axis. The distance from a node to the center and the velocities relative to this center are then calculated according to the methods presented in Sec. III D.

C. Numerical integration and interpretation of the results

As a specific example, the initial time $t_{\rm in}$ is taken to correspond to the redshift $z_{\rm in}\equiv a(t_0)/a(t_{\rm in})-1=50$, considering the final time t_0 of the integration as the "present time" ($z=0$). The initial conditions are completely specified by the value of ϵ, while the physical length scale attached to R_V would fix the astrophysical problem under consideration; we considered the two cases $\epsilon=1.87\times10^{-2}$ (case I) and $\epsilon=3.3\times10^{-2}$ (case II). In both cases we shall present results obtained with

$R_V = 0.43h^{-1}$ Mpc (h being the Hubble constant in units of 100 km s^{-1} Mpc^{-1}). Case I leads to a final value of the central density contrast $\delta_c \simeq 3$, representing a situation of mildly nonlinear evolution, while case II, for which $\delta_c \simeq 650$, allows to test our method in a fully nonlinear situation.

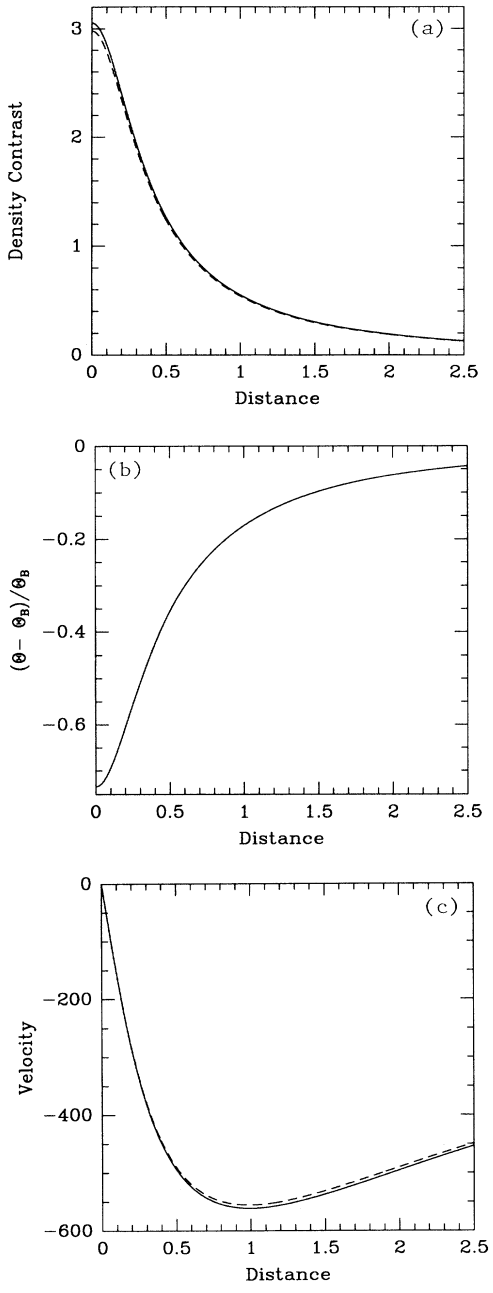

FIG. 1. Results obtained in the numerical integration (dashed lines) for some representative fluid quantities are compared with those given by the exact Tolman-Bondi solution (solid lines) for case I. Quantities are plotted as functions of the proper distance from the origin given in units of $R_V(a_0/a_{\rm in})$. (a) Density contrast. (b) Relative change of expansion with respect to the background value. (c) Peculiar radial velocity (km s^{-1}) relative to the origin.

The numerical integration has been carried out over $N_g = 1000$ nodes, conveniently spaced from the origin to $2.5R_V$, with a higher density of grid points near the center. The set of equations A was solved along the world line of each fluid element using a fourth-order Runge-Kutta method. Let us note that the Cartesian axis (x^3 in our case) on which all grid points have been taken coincides with one of the principal axes of both $\sigma^\alpha{}_\beta$ and $E^\alpha{}_\beta$. Because of the zero trace constraint, only two of the three distinct eigenvalues of each tensor need to be integrated, while the third can be computed from the oth-

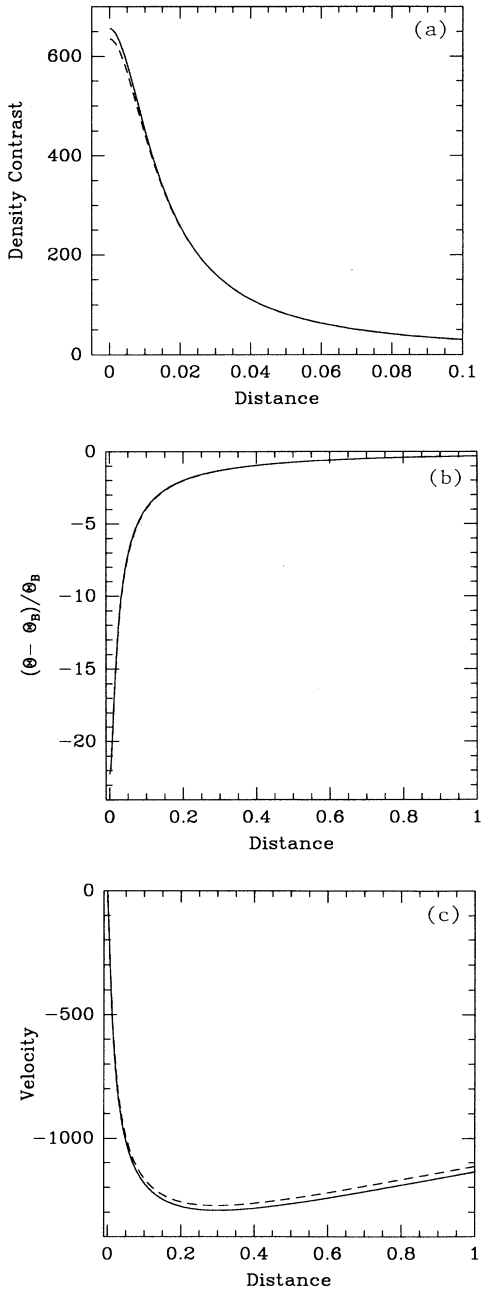

FIG. 2. Same as in Fig. 1, but for case II.

ers. Actually, thanks to the spherical symmetry, for any point lying on our radial axis there is only one independent eigenvalue for the shear and one for the tidal force field, $\sigma_1=\sigma_2$ and $E_1=E_2$ (see also Sec. V). However, in the present work, we are also interested in checking the accuracy of the numerical solution, and so we preferred to integrate all of the components of the shear and tidal force fields and use the corresponding constraint equations to check the accuracy of the code. The numerical results show that these are satisfied better than 1 part in 10^{10} for σ_{ab} and 1 part in 10^{12} for E_{ab} in both cases. The relative radial distances between the nodes and their velocities were finally computed from Eqs. (3.14)–(3.16).

Figure 1 shows some relevant fluid quantities for case I at the present time: It shows the density contrast, the relative change of the expansion scalar with the respect to the background value, $(\Theta-\Theta_B)/\Theta_B$, and the peculiar radial velocity from the center computed according to our algorithm, as functions of the Eulerian radial distance from the origin in units of $R_V(a_0/a_{\rm in})$. Figure 2 shows the same quantities but for case II. The comparison with the TB profiles computed from the exact solution shows very good agreement both in cases I and II. The difference in the velocity curve between the exact and numerical solutions is related to the grid resolution. We have verified that by doubling the number of grid points, the difference between the two curves is halved. Finally, similar curves obtained for other scalar quantities, such as σ^2, $E_{ab}E^{ab}$, and $\sigma_{ab}E^{ab}$, in the numerical integration are completely indistinguishable from the exact solution in both cases.

V. EXACT SOLUTIONS: THE PLANAR SYMMETRIC CASE

In the system (3.12), the FRW background expansion can be factored out, which turns out to be particularly useful when looking for exact solutions. We then define the comoving density $1+\delta\equiv\rho/\rho_B$, where δ represents the fractional density fluctuation, the scaled peculiar expansion $\vartheta\equiv(1/\dot a)(\Theta-\Theta_B)$, shear eigenvalues $s_\alpha\equiv(1/\dot a)\sigma_\alpha$, and, finally, the scaled eigenvalues of the tidal force tensor, $e_\alpha\equiv(t/\dot a)E_\alpha$. It will also prove convenient to use as time variable the scale factor $a(t)$ itself. The system (3.12) reduces to

$$
\begin{aligned}
\delta' &= -(1+\delta)\vartheta \ , \\
\vartheta' &= -\frac{3}{2a}\vartheta-\frac{1}{3}\vartheta^2-2(s_1^2+s_2^2+s_1s_2)-\frac{3}{2a^2}\delta \ , \\
s_1' &= -\frac{3}{2a}s_1-\frac{1}{3}s_1(s_1+2\vartheta)+\frac{2}{3}s_2(s_1+s_2) \\
&\quad -\frac{3}{2a}e_1 \ , \\
s_2' &= -\frac{3}{2a}s_2-\frac{1}{3}s_2(s_2+2\vartheta)+\frac{2}{3}s_1(s_2+s_1) \\
&\quad -\frac{3}{2a}e_2 \ ,
\end{aligned}
\tag{5.1}
$$

$$
\begin{aligned}
e_1' &= -\frac{1}{a}e_1+e_1(s_1-s_2-\vartheta)-e_2(s_1+2s_2) \\
&\quad -\frac{1}{a}(1+\delta)s_1 \ , \\
e_2' &= -\frac{1}{a}e_2+e_2(s_2-s_1-\vartheta)-e_1(s_2+2s_1) \\
&\quad -\frac{1}{a}(1+\delta)s_2 \ ,
\end{aligned}
$$

where the prime denotes differentiation with respect to a. The initial conditions read

$$
\begin{aligned}
\delta_{\rm in} &= -a_{\rm in}\vartheta_{\rm in}=a_{\rm in}(\lambda_1+\lambda_2+\lambda_3) \ , \\
s_{1\rm in} &= -e_{1\rm in}=-\tfrac{1}{3}(2\lambda_1-\lambda_2-\lambda_3) \ , \\
s_{2\rm in} &= -e_{2\rm in}=-\tfrac{1}{3}(2\lambda_2-\lambda_1-\lambda_3) \ .
\end{aligned}
\tag{5.2}
$$

Note that, in the limit $a_{\rm in}\to 0$ at finite φ, the fluid starts with uniform density, $\delta_{\rm in}=0$.

The comoving relative displacements along the local principal axes y_α evolve according to

$$
y_\alpha'=(s_\alpha+\tfrac{1}{3}\vartheta)y_\alpha \ ,
\tag{5.3}
$$

while the components of the physical relative peculiar velocity correspond to $v^\alpha=a\dot a y_\alpha'$ (the rotation to principal axes and its inverse are clearly not affected by our rescaling). Particularly interesting is the case in which two eigenvalues, say, λ_1 and λ_2, are equal, this being both the case of spherical and planar symmetries. In the spherically symmetric case, $\varphi=\varphi(r)$, giving $\lambda_1=\lambda_2=r^{-1}d\varphi/dr$ and $\lambda_3=d^2\varphi/dr^2$, for any point lying on the x^3 axis. The case of symmetry on the (x^1,x^2) plane corresponds to $\lambda_1=\lambda_2=0$. In both cases one clearly has $s_1=s_2\equiv s$ and $e_1=e_2\equiv e$ at all times and the system (5.1) is further simplified to

$$
\begin{aligned}
\delta' &= -(1+\delta)\vartheta \ , \\
\vartheta' &= -\frac{3}{2a}\vartheta-\frac{1}{3}\vartheta^2-6s^2-\frac{3}{2a^2}\delta \ , \\
s' &= -\frac{3}{2a}s+s^2-\frac{2}{3}s\vartheta-\frac{3}{2a}e \ , \\
e' &= -\frac{1}{a}e-e\vartheta-3es-\frac{1}{a}(1+\delta)s \ .
\end{aligned}
\tag{5.4}
$$

In what follows we shall only consider the planar symmetric case. In such a case, the absence of perturbations on the (x^1,x^2) plane implies that $s=-\frac{1}{3}\vartheta$. One immediately gets the following solution, along a fluid trajectory:

$$
\begin{aligned}
1+\delta(q,t) &= \frac{1+a_{\rm in}\lambda_3(q)}{1-\tau\lambda_3(q)} \ , \\
\vartheta(q,t) &= -\frac{\lambda_3(q)}{1-\tau\lambda_3(q)} \ , \\
s(q,t) &= \frac{1}{3}\,\frac{\lambda_3(q)}{1-\tau\lambda_3(q)} \ , \\
e(q,t) &= -\frac{1}{3}\,\frac{\lambda_3(q)}{1-\tau\lambda_3(q)} \ ,
\end{aligned}
\tag{5.5}
$$

where q is the Lagrangian (i.e,. initial) comoving (with respect to FRW space-time) longitudinal coordinate labeling the fluid element and $\tau \equiv a - a_{\rm in}$. This solution is valid up to the first orbit crossing, which occurs at the "time" $\tau_c = 1/\lambda_3(q)$, for $\lambda_3 > 0$ (i.e., for initially overdense regions). The infinitesimal Eulerian distance between neighboring elements is easily obtained from Eq. (3.13):

$$dy = [1 - \lambda_3(q)\tau]dq \ . \tag{5.6}$$

This can be integrated to give the finite distance between two points O and S,

$$y_S - y_O = q_S - q_O - \tau \int_{q_O}^{q_S} dq \ \lambda_3(q) \ , \tag{5.7}$$

or, recalling that $\lambda(q) = d^2\varphi/dq^2$,

$$y(q,\tau) = q - \tau \frac{d\varphi(q)}{dq} \ . \tag{5.8}$$

This solution is identical to the well-known Zel'dovich one [8] for the Newtonian case. It is, however, worth noting that in deriving Eq. (5.7) some of the curvature effects were disregarded. The peculiar velocity of the fluid element q (i.e., the velocity with respect to the FRW background after Hubble flow subtraction) is immediately obtained from Eq. (5.8) [or from Eq. (5.7) by the method described in Sec. III D]:

$$v[y(q,t)] = -a\dot{a} \frac{d\varphi(q)}{dq} \ , \tag{5.9}$$

where $t = t_{\rm in}(1 + \tau/a_{\rm in})^{3/2}$. This analytical solution also allows one to check that the physical distance between neighboring nodes remains smaller than the local curvature length

$$1/[|\mathcal{R}^{(3)}(q,t)|]^{1/2} = [9t^2/40|\delta(q,t)|]^{1/2}$$

during the evolution, provided it was so initially.

In this case the planar symmetry of the system implies that the magnetic part of the Weyl tensor, H_{ab}, identically vanishes during the whole evolution, and so our solution of Eqs. (5.5) and (5.6) is exact.

VI. DISCUSSION AND CONCLUSIONS

In this work we have proposed a GR approach to the fully three-dimensional nonlinear evolution of a self-gravitating collisionless fluid up to the epoch of first caustic formation. Our method relies on the approximation of neglecting the interaction for gravitational waves with the rest of the system. Also, we assume that the fluid motion is irrotational. Under these assumptions a simple Lagrangian picture is obtained, which, after self-consistent initial conditions have been assigned to an initial grid, allows one to follow the evolution for each fluid element (grid node) separately in its own local inertial rest frame. This method has two evident advantages: First, being Lagrangian, it automatically guarantees enhanced resolution in regions of higher density, i.e., where it is more needed; second, it allows one to follow each fluid element as being completely independent of the others, which obviously reduces the amount of computer storage needed to evolve the system. Only at the initial time should the conditions be specified simultaneously on the whole grid, and this requires an amount of computer memory comparable to the one required to construct the initial conditions in an N-body code. For instance, if we consider an initial random (e.g., Gaussian) realization of the peculiar gravitational potential in momentum space, $\hat{\varphi}(\mathbf{k})$ (e.g., for a given choice of its power spectrum), initial conditions on the grid should be obtained by inverse Fourier transforming the symmetric tensor $k_\alpha k_\beta \hat{\varphi}(\mathbf{k})$. A clear advantage of our method is then that it allows one to concentrate on the evolution for a given region, where structures are forming, while its gravitational interaction with the rest of the universe has been already included by the setup of the initial conditions.

The choice of a pressureless fluid and the approximation of disregarding gravitational waves have partially limited the occurrence of truly relativistic effects in our problem: These would show up, for instance, as finite-distance effects through the curvature of comoving hypersurfaces and through the relativistic velocities of fluid elements with horizon-size distance, although these effects have been partially hidden by our approach to obtain the Eulerian representation of the results. Our final picture has been constructed on a fixed synchronous-time hypersurface; however, one could also figure out how to implement our algorithm in order to reproduce the matter distribution as seen by a comoving observer in his past light cone.

It is clearly important to understand how to follow the evolution of the system in the multistream regions which occur after caustic formation. The occurrence of caustics is indicated by the vanishing of the distance δl between neighboring elements or by the local divergence of the density. In the literature several semianalytical methods have been developed in order to follow the evolution in the early nonlinear phases or to reconstruct the initial conditions of the clustering process. Most of these methods try to circumvent caustic formation: This can be obtained either by suitable smoothing procedures (e.g., Ref. [30]), or by artificially sticking the particles as their orbits first cross [9], or by asymptotically slowing down particle motions so that orbit mixing never occurs [13]. Also, one could consider the possibility of replacing the *fluid* approximation with the more realistic picture of a system of noninteracting particles. An extension of our method, dealing with the problem of orbit crossing, will be the subject of future investigation.

ACKNOWLEDGMENTS

We would like to acknowledge Ed Bertschinger and Marco Bruni for helpful discussions. This work has been partially supported by Italian MURST. D.S. thanks the Conselleria de Cultura, Educacio i Ciencia de la Generalitat Valenciana and the Spanish DGICYT Project No. PB90-0416 for financial support.

[1] E. M. Lifshitz, J. Phys. (Moscow) **10**, 116 (1946).
[2] S. W. Hawking, Astrophys. J. **145**, 544 (1966).
[3] J. M. Bardeen, Phys. Rev. D **22**, 1882 (1980).
[4] E. T. Vishniac, Astrophys. J. **257**, 456 (1982); R. K. Schaefer, Int. J. Mod. Phys. A **6**, 2075 (1991).
[5] T. Futamase, Phys. Rev. Lett. **61**, 2175 (1988).
[6] P. J. E. Peebles, *The Large Scale Structure of the Universe* (Princeton University Press, Princeton, 1980).
[7] R. C. Tolman, Proc. Natl. Acad. Sci. **20**, 169 (1934); H. Bondi, Mon. Not. R. Astron. Soc. **107**, 410 (1947).
[8] Ya. B. Zel'dovich, Astrophysica **6**, 160 (1970); Astron. Astrophys. **5**, 84 (1970).
[9] S. N. Gurbatov, A. I. Saichev, and S. F. Shandarin, Mon. Not. R. Astron. Soc. **236**, 385 (1980); L. A. Kofman, D. Yu. Pogosyan, and S. F. Shandarin, *ibid.* **242**, 200 (1990).
[10] A. Nusser, A. Dekel, E. Bertschinger, and G. R. Blumenthal, Astrophys. J. **379**, 6 (1991); A. Nusser and A. Dekel, *ibid.* **391**, 443 (1992); M. Giavalisco, B. Mancinelli, P. Mancinelli, and A. Yahil, report, 1991 (unpublished); M. Gramann, Astrophys. J. (to be published).
[11] F. Moutarde, J.-M. Alimi, F. R. Bouchet, R. Pellat, and A. Ramani, Astrophys. J. **382**, 377 (1991).
[12] A. Yahil, report, 1991 (unpublished).
[13] S. Matarrese, F. Lucchin, L. Moscardini, and D. Saez, Mon. Not. R. Astron. Soc. **253**, 437 (1992).
[14] R. W. Hockney and J. W. Eastwood, *Computer Simulations using Particles* (McGraw-Hill, New York, 1981).
[15] P. J. E. Peebles, Astrophys. J. **317**, 576 (1987).
[16] J. A. Fillmore and P. Goldreich, Astrophys. J. **281**, 1 (1984); **281**, 9 (1984); E. Bertschinger, Astrophys. J. Suppl. **58**, 1 (1985); **58**, 39 (1985); R. N. Henriksen, Mon. Not. R. Astron. Soc. **240**, 917 (1989).
[17] M. E. Cahill and A. H. Taub, Commun. Math. Phys. **21**, 1 (1971); B. J. Carr and A. Yahil, Astrophys. J. **360**, 330 (1990); J. Ponce de Leon, Mon. Not. R. Astron. Soc. **250**, 69 (1991).
[18] O. M. Blaes, P. M. Goldreich, and J. V. Villumsen, Astrophys. J. **361**, 331 (1990).
[19] K. A. Olive, Phys. Rep. **190**, 307 (1990); V. F. Mukhanov, H. A. Feldman, and R. H. Brandenberger, *ibid.* **215**, 203 (1992).
[20] C. M. Lewis, Phys. Rev. D **44**, 1661 (1991).
[21] V. Sahni, Phys. Rev. D **42**, 453 (1990).
[22] S. Matarrese, Proc. R. Soc. London **A401**, 53 (1985).
[23] L. Kofman, in *Primordial Nucleosynthesis and Evolution of the Early Universe,* Proceedings of the IUPAP Conference, Tokyo, Japan, 1990, edited by K. Sato (Kluwer Academic, Dordrecht, 1991).
[24] T. Buchert, Astron. Astrophys. **223**, 9 (1989); Mon. Not. R. Astron. Soc. **254**, 729 (1992).
[25] F. R. Bouchet, R. Juszkiewicz, S. Colombi, and R. Pellat, Astrophys. J. Lett. **394**, L5 (1992).
[26] G. F. R. Ellis, in *General Relativiity and Cosmology,* edited by R. K. Sachs (Academic, New York, 1971).
[27] M. Bruni, P. K. S. Dunsby, and G. F. R. Ellis, Astrophys. J. **395**, 34 (1992).
[28] D. S. Salopek and J. R. Bond, Phys. Rev. D **42**, 3936 (1990); D. S. Salopek, *ibid.* **43**, 3214 (1991).
[29] A. Barnes and R. R. Rowlingson, Class. Quantum Grav. **6**, 949 (1989); we thank M. Bruni for driving our attention to this reference.
[30] A. Dekel, E. Bertschinger, and S. M. Faber, Astrophys. J. **364**, 349 (1990).
[31] D. W. Olson, Phys. Rev. D **14**, 327 (1976).
[32] D. H. Lyth and M. Mukherjee, Phys. Rev. D **38**, 485 (1988); D. H. Lyth and E. D. Stewart, Astrophys. J. **361**, 343 (1990).
[33] G. F. R. Ellis and M. Bruni, Phys. Rev. D **40**, 1804 (1989); G. F. R. Ellis, J. Hwang, and M. Bruni, *ibid.* **40**, 1819 (1989).
[34] J. Hwang, Astrophys. J. **380**, 307 (1991); J. Hwang and E. T. Vishniac, *ibid.* **353**, 1 (1990).
[35] S. Weinberg, *Gravitation and Cosmology* (Wiley, New York, 1972).
[36] F. J. Tipler, C. J. S. Clarke, and G. F. R. Ellis, in *General Relativity and Gravitation,* edited by A. Held (Plenum, New York, 1980).
[37] M. Panek, Astrophys. J. **388**, 225 (1992).
[38] J. V. Arnau, M. J. Fullana, L. Monreal, and D. Saez, Astrophys. J. (to be published).
[39] C. Hellaby and K. Lake, Astrophys. J. **290**, 381 (1985); A. Mészáros, Mon. Not. R. Astron. Soc. **253**, 619 (1991).